The phosphoinositide phosphatase MTM-1 regulates apoptotic cell corpse clearance through CED-5–CED-12 in C. elegans

Lukas Jakob Neukomm[1,*], Anne-Sophie Nicot[2,†], Jason Michael Kinchen[1,‡], Johann Almendinger[1], Sérgio Morgado Pinto[1], Sheng Zeng[1], Kimon Doukoumetzidis[1], Hélène Tronchère[3], Bernard Payrastre[3], Jocelyn Franck Laporte[2] and Michael Otmar Hengartner[1,§]

SUMMARY

Multicellular organisms use programmed cell death to eliminate unwanted or potentially harmful cells. Improper cell corpse removal can lead to autoimmune diseases. The development of interventional therapies that increase engulfment activity could represent an attractive approach to treat such diseases. Here, we describe mtm-1, the Caenorhabditis elegans homolog of human myotubularin 1, as a potential negative regulator of apoptotic cell corpse clearance. Loss of mtm-1 function leads to substantially reduced numbers of persistent cell corpses in engulfment mutants, which is a result of a restoration of engulfment function rather than of impaired or delayed programmed cell death. Epistatic analyses place mtm-1 upstream of the ternary GEF complex, which consists of ced-2, ced-5 and ced-12, and parallel to mig-2. Over-activation of engulfment results in the removal of viable cells that have been brought to the verge of death under limiting caspase activity. In addition, mtm-1 also promotes phagosome maturation in the hermaphrodite gonad, potentially through CED-1 receptor recycling. Finally, we show that the CED-12 PH domain can bind to PtdIns(3,5)P_2 (one target of MTM-1 phosphatase activity), suggesting that MTM-1 might regulate CED-12 recruitment to the plasma membrane.

KEY WORDS: Apoptosis, Cell death, Phagocytosis, Caenorhabditis elegans

INTRODUCTION

Tissue homeostasis and organ formation requires a physiological balance that regulates proliferation and death of cells (Hanahan and Weinberg, 2000). Once a single cell is committed to die, neighboring or specialized phagocytic cells recognize, internalize and degrade the cell corpse. Cell corpse clearance ensures that corpses are not able to release harmful intracellular contents into the surrounding tissue, which could evoke inflammation and autoimmune disease (Nagata et al., 2010; Savill and Fadok, 2000).

In the nematode Caenorhabditis elegans, greater than 20 genes involved in the recognition, internalization and degradation of apoptotic cell corpses have been described. Loss-of-function (lf) alleles of these genes result in the accumulation of persistent cell corpses in the soma and/or in the hermaphrodite gonad. Genetic and biochemical analyses placed the engulfment genes in three partially redundant pathways that might converge at the level of the small GTPase CED-10 (Rac1 in mammals), which is followed by a 'linear' phagosome maturation pathway that is required for the degradation of engulfed cell corpses (Fullard et al., 2009; Kinchen, 2010).

In a first pathway, CED-7 (ABCA1) and CED-1 (MEGF10) have been proposed to function as receptors for the recognition of dying cells, either directly, or via the bridging molecule TTR-52 (Wang et al., 2010; Wu and Horvitz, 1998b; Zhou et al., 2001b). The adaptor protein CED-6 (GULP) physically binds to and might transduce signal(s) from CED-1 further downstream to the small GTPase CED-10, and additionally regulates phagosome maturation through the large GTPase DYN-1 (Dynamin) (Kinchen et al., 2005; Liu and Hengartner, 1998; Yu et al., 2006).

In a second signaling cascade, two small Rho GTPases act in a serial manner: UNC-73 (Trio) acts as a guanosine exchange factor (GEF) for the small GTPase MIG-2 (RhoG) (deBakker et al., 2004). Active (i.e. GTP-loaded) MIG-2 regulates corpse removal by modulating plasma membrane recruitment of the unconventional bipartite CED-5 (Dock180)–CED-12 (Elmo) GEF complex (Gumienny et al., 2001; Wu and Horvitz, 1998a). The GEF complex is stabilized further by the adaptor molecule CED-2 (CrkII), which also promotes the activation of CED-10 (Akakura et al., 2005; Gumienny et al., 2001). GTP-bound CED-10 initiates extensive cytoskeletal rearrangements, a requirement for the engulfment of cell corpses (Kiyokawa et al., 1998; Reddien and Horvitz, 2000).

Several receptors in the second signaling pathway have been described, with MOM-5 (Frizzled) proposed to act as the major receptor important for embryonic corpse recognition, signaling

[1]Institute of Molecular Life Science, University of Zürich, Winterthurerstrasse 190, 8057 Zürich, Switzerland. [2]Department of Translational Medecine and Neurogenetics, Institut de Génétique et de Biologie Moléculaire et Cellulaire (IGBMC), Institut National de la Santé et de la Recherche Médicale U964, Centre National de la Recherche Scientifique Unité Mixte de Recherche 7104, Université de Strasbourg, Collège de France, 67404 Illkirch, France. [3]INSERM, U1048, Université Toulouse III Paul Sabatier, I2MC, CHU de Toulouse, Laboratoire d'Hématologie, 31432 Toulouse cedex 4, France.

*Present address: Department of Neurobiology, Howard Hughes Medical Institute, University of Massachusetts Medical School, Worcester, MA 01605, USA
†Present address: Laboratoire de Biologie Moleculaire et Cellulaire, Centre National de la Recherche Scientifique, Unite Mixte de Recherche 5239, Ecole Normale Superieure de Lyon, Universite Lyon 1, 69364 Lyon, France
‡Present address: Center for Cell Clearance and Department of Microbiology, University of Virginia, Charlottesville, VA 22903, USA
§Author for correspondence (michael.hengartner@imls.uzh.ch)

Accepted 8 February 2011

through GSK-3 (GSK3β), APR-1 (APC) and CED-2 to activate CED-10, providing a link between corpse recognition and activation of CED-10 (Cabello et al., 2010). Additionally, the two integrins INA-1 (Integrin α) and PAT-3 (Integrin β) play a redundant role in corpse recognition and might also recruit CED-2 to the phagocytic cup in a phosphotyrosine-dependent manner through SRC-1 (Src) (Hsu and Wu, 2010).

A third pathway has been described in which ABL-1 (Abl kinase) regulates cytoskeletal remodeling through ABI-1 (Abi), potentially through CED-10 and in a yet unknown CED-10-independent way (Hurwitz et al., 2009).

Once CED-10 is activated, downstream signaling towards the cytoskeleton will lead to an extensive re-orchestration within the phagocytic cell. As a result, the cell corpse will be fully internalized and its components will be degraded and recycled (Kinchen, 2010; Nagata et al., 2010). Following corpse internalization, the GTPase activating protein (GAP) SRGP-1 inactivates CED-10, thereby turning engulfment signaling off (Neukomm et al., 2011).

Cytoskeletal rearrangements are associated with altered membrane dynamics on the plasma membrane (Saarikangas et al., 2010). Polyphosphoinositides (PPIn), phosphorylated derivatives of phosphatidylinositol (PtdIns) (see Mitchell et al., 2006), are the most versatile and crucial regulators of cytoskeletal dynamics, signal transduction, membrane trafficking and phagosome formation (Simonsen et al., 2001; Yeung et al., 2006). Interestingly, several proteins involved in corpse removal were shown to contain features predicted to bind phospholipids. For example, the mammalian CED-5 ortholog, Dock180 (now known as Dock1), binds $PtdIns(3,4,5)P_3$ and $PtdIns(3,5)P_2$ via its DHR1 domain. However, only a limited number of kinases and phosphatases linking PPIn to phagocytosis of apoptotic cells have been described (Leverrier et al., 2003; Liu et al., 2005; Zou et al., 2009).

In this paper, we present a genetic screen that allowed us to identify 13 new mutations that enhance cell corpse clearance in *C. elegans*. We show that the strongest suppressor mutation is a viable, hypomorphic allele of *mtm-1*, a PPIn phosphatase identified independently by Zou et al. in an RNAi screen for negative regulators of cell corpse clearance (Zou et al., 2009). Using our allele, we confirm that MTM-1 functions upstream of the CED-5–CED-12 GEF for CED-10, and show that MTM-1 acts in parallel to MIG-2 in the regulation of this GEF complex. We demonstrate that MTM-1, similar to its human homolog myotubularin 1, has biochemical phosphatase activity towards both $PtdIns3P$ and $PtdIns(3,5)P_2$, and that expression of the human homolog can rescue the *C. elegans* mutant phenotype. Finally, we show that, in addition to its negative regulation of corpse internalization, MTM-1 function is required for proper maturation of phagosomes containing cell corpses and for recycling of CED-1 back to the plasma membrane. Our findings suggest that during internalization MTM-1 modulates CED-10 activity by controlling the amount of plasma membrane $PtdIns(3,5)P_2$, which provides docking sites for the recruitment and/or activation of the CED-5–CED-12 GEF complex. Later, during phagosome maturation, MTM-1 might act on the same lipid intermediates to control CED-1 receptor recycling.

MATERIALS AND METHODS
Mutations and strains
C. elegans strains were grown at 20°C as described previously (Brenner, 1974). The wild-type strain used was Bristol N2. The following alleles were used: LGI: *mtm-1(op309)*, *mtm-1(ok742)*, *gla-1(op234)*, *ced-*

12(k149), *ced-12(bz187)*, *ced-12(oz167)*, *ced-1(e1735)* and *ced-1(n1995)*. LGIII: *ced-6(n1813)*, *ced-6(tm1826)*, *ced-6(op360)*, *ced-7(n1892)*, *ced-7(n1996)*, *ced-7(n2690)* and *unc-119(ed3)*. LGIV: *ced-2(n1994)*, *ced-2(e1752)*, *ced-10(n3246)*, *ced-10(n1993)*, *ced-5(n1812)*, *ced-5(tm1949)*, *ced-5(n2002)*, *ced-3(n2433)*, *ced-3(n717)* and *ced-3(op149)*. LGX: *mig-2(mu28)*, *mig-2(gm103gf)* and *dyn-1(n4039)*. All alleles are described in WormBase (http://www.wormbase.org/).

Integrated arrays [containing *unc-119-(+)*] used were: *opIs110[P_ced-1::yfp::act-5]*, *opIs195[P_mtm-1(short)::yfp::mtm-1(genomic)]*, *opIs220[P_eft-3::dyn-1(genomic)::yfp]*, *opIs222[P_eft-3::gfp::fyve::fyve]*, *opIs265[P_mtm-1(long)::cfp::mtm-1(genomic)]*, *opIs266[P_mtm-1(long)::yfp::mtm-1(op309,genomic)]*, *opIs282[P_ced-1::yfp::rab-5]*, *opIs334 [P_ced-1::yfp::fyve::fyve]* *nIs96[P_lin-11::gfp; lin-15(+)]* and *bcIs39[P_lim-7::ced-1::gfp; lin-15(+)]*. Extrachromosomal arrays used were: *opEx1280[P_mtm-1(long)::gfp::hmtm1(cDNA); unc-119(+)]*, *opEx1303[P_ced-1::yfp::rab-7; unc-119(+)]* and *opEx1465[P_lst-4::lst-4c(genomic)::yfp; unc-119(+)]*. Balancers were: *szT1[lon-2(e678)] (I;X)*.

ENU Mutagenesis
Staged L4 *gla-1(op234); ced-6(n1813)* mutants were mutagenized [1 mM N-ethyl-N-nitrosourea (ENU) in M9 for 4 hours] and allowed to recover overnight at 15°C (De Stasio and Dorman, 2001). Worms were transferred to plates to lay eggs for 4-6 hours at 20°C, then burned off; ~3 days later (when F1 progeny had reached adulthood) adults were counted and removed. F2 progeny were incubated for 24-36 hours post-L4/adult molt and stained with Acridine Orange (AO) as described previously (Kinchen et al., 2005; Neukomm et al., 2011).

Mapping *op309*
For two-factor mapping, *op309* males were crossed into mapping triples (*dpy-5* I; *rol-6* II; *lon-1* III or *unc-5* IV; *dpy-11* V; *lon-2* X) and F2 homozygote *op309* hermaphrodites were tested for segregated markers in the F3 generation (AO staining in a *gla-1; ced-6* background). Homozygote *dpy-5* mutants were never observed indicating tight linkage to the middle of chromosome I.

For three-factor mapping, *op309* was mapped onto the *unc-74 dpy-5* genomic segment, closer to the left side, as 11 out of 15 Unc-non-Dpy worms and five out of 15 Dpy-non-Unc worms were suppressed by *op309* (corpse numbers in L1 heads in a *ced-6* background). This interval contains 203 genes.

For sequencing, *mtm-1(op309)* animals contain a G to A substitution (introducing an *Eco*RI site) in exon 4 compared with wild type.

RNA interference (RNAi) by feeding
RNAi was performed as described previously (Kamath and Ahringer, 2003; Neukomm et al., 2011). Among all 203 candidate genes tested, AO+ germ cell corpses reappeared solely in *mtm-1(RNAi)*-treated animals.

Phenotypic analysis
For embryonic apoptotic cell corpses, mixed embryos were mounted on a 3% agar pad and indicated stages scored for persistent cell corpse in whole bodies using a differential interference contrast (DIC) microscope. Larval L1 head apoptotic cell corpses: Scores were performed as described (Neukomm et al., 2011). For germ cell corpses, >20 either 12, 24 or 36 hour post-L4/adult molts were mounted (3% agar) and anesthetized (5 mM levamisole in M9). Refractive apoptotic germ cell corpses were scored using a DIC microscope and, if applicable, by fluorescent halo scoring using an epifluorescence microscope.

For P*n*.aap cell survival, P*n*.aap cells were scored as described previously (Reddien et al., 2001).

Total RNA isolation and cDNA synthesis
RNA isolation and cDNA synthesis was performed as described previously (Neukomm et al., 2011).

Generation of transgenic strains
Transgenic worms were generated as described previously (Kinchen et al., 2005; Neukomm et al., 2011).

Table 1. Plasmids used in this study

Plasmid name	Description	Used for
pLN041	*P_mtm-1(short)::yfp::mtm-1(genomic); unc-119(+)*	*opIs195*
pLN128	*P_mtm-1(long)::cfp::mtm-1(genomic); unc-119(+)*	*opIs265*
pLN130	*P_mtm-1(long)::yfp::mtm-1(op309,genomic); unc-119(+)*	*opIs266*
pLN132	*P_mtm-1(long)::gfp::hmtm1(cDNA); unc-119(+)*	*opEx1280*
pLN126	pL4440 Y48G1C.10	*mtm-12* (clone I) RNAi
pLN127	pL4440 Y48G1C.11	*mtm-12* (clone II) RNAi
pLN219	pL4440 empty	Empty vector RNAi
pLN230	pDEST15 gst::ph(ced-12)	In vitro dot blots
pLN226	pDEST15 gst	In vitro dot blots
mtm-1.FL.WT	pENTR1A mtm-1(cDNA)	Gateway entry vector
mtm-1.FL.G106E	pENTR1A mtm-1(op309, cDNA)	Gateway entry vector
mtm-1.WT	pDEST15 gst::mtm-1(cDNA)	Phosphatase activity tests
mtm-1.G106E	pDEST15 gst::mtm-1(op309,cDNA)	Phosphatase activity tests

4D microscopy, lineaging and cell corpse persistence measurement
Fertilized single-cell eggs were isolated, mounted on a coverslide (containing 0.1% poly-L-lysine) in M9 and sealed with vaseline. Using OpenLab Imaging software and a Leica DMR-A2 DIC microscope, 40 z-stack pictures ($\approx$0.8 µm distance) through the embryo were taken every 30 seconds for 7 hours. The first 12 apoptotic cells in the AB lineage were followed using Virtual Wormbase (http://www.biosci.ki.se/groups/tbu/software) using tiff files. Onset of cell death was defined as the time between single-cell embryo (t_{1-cell}) and cell death (onset of refractivity, t_{lentil}), i.e. $t_{lentil} - t_{1-cell}$. Corpse persistence was defined as the time between onset of death (t_{lentil}) and cleared corpse ($t_{engulfed}$), i.e. $t_{engulfed} - t_{lentil}$ (Hoeppner et al., 2001).

3-phosphate phosphatase assay
Recombinant GST::MTM-1 proteins (wild-type and G106E) were expressed in *E. coli* CodonPlus BL21 bacteria, lysed by sonication (lysis buffer: 10 mM Tris, 50 mM NaCl, 50 mM KCl, 10% glycerol, 1 mM DTT, 100 ng/µl lysozyme, PIC, pH 7.0), centrifuged (10,000 ***g*** for 10 minutes) and purified with glutathione Sepharose 4B beads (GE Healthcare) in lysis buffer containing 1% Triton for 2 hours. Recombinant proteins were washed (10 mM Tris, 50 mM NaCl, 50 mM KCl, 10% glycerol, 0.1% NP40, 1 mM DTT, pH 7), eluted (100 mM Tris, 150 mM NaCl, 30 mM glutathion, pH 7) and dialysed (10 mM Tris, 50 mM NaCl, 50 mM KCl, 10% glycerol, pH 7).

Phosphatase activity using fluorescent substrate was performed as described previously (Rohde et al., 2009) with slight modifications. Increasing concentrations of recombinant proteins were incubated with 2.5 µg of C6-BODIPY-FL-PtdIns3*P* or C6-BODIPY-FL-PtdIns(3,5)*P*₂ (Echelon Bioscience) in 50 mM ammonium acetate, pH 6.0 (30°C, 30 minutes) and the reaction stopped with chloroform/methanol (1/1). Fluorescent lipids (upper phase) were dried (nitrogen), resuspended [methanol/isopropanol/acetic acid (5/5/2)], separated by thin-layer chromatography [chloroform/methanol/acetone/acetic acid/water (7/5/2/2/2)] and visualized under ultraviolet light.

PtdIns3*P* confocal microscopy
L2 larvae were mounted (2% agarose) in 0.2% NaN₃ in M9. Images were taken with a Zeiss LSM710 confocal microscope and GFP::FYVE::FYVE punctae scored with ImageJ (NIH), n=25.

Lipid dot blots
GST or GST::PH_CED-12 were expressed in BL21(DE3) CodonPlus bacteria (Stratagene) at 4°C overnight, then harvested as described previously (Kinchen et al., 2008). Lipid dot blots (Echelon Bioscience) were incubated with ~1.0 µg/ml of protein overnight, then developed as described previously (Park et al., 2007).

Transmission electron microscopy
Worms were high-pressure frozen (EM Pact2, Leica Microsystems) using flat specimen carriers (indentation, 1.5 mm×0.2 mm). The hole of the carrier (dedicated for pressure transmission) was filled with 1-hexadecene and the cavity of the carrier with a droplet of PBS. Worms were transferred to the PBS droplet, and the majority of PBS was drawn off (filter paper)

leaving the worms in a small PBS volume. 1-Hexadecene was added (on top), the specimen immediately frozen and freeze-substituted in anhydrous acetone containing 2% OsO₄ (Leica EM AFS2). Specimens were kept successively at –90°C, –60°C, and –30°C (8 hours each), then changed at a rate of 30°C per hour to reach room temperature, (RT). After 1 hour, OsO₄ was removed with anhydrous acetone and the specimens gradually embedded in 33% Epon/Araldite (EA) in anhydrous acetone (overnight, 4°C), 66% EA in anhydrous acetone (6 hours, 4°C) and 100% EA (1 hour, RT) prior to polymerization (60°C, 48 hours). Thin sections were stained with aqueous 2% uranyl acetate and Reynolds lead citrate and imaged (Phillips CM 100 TEM, FEI, Netherlands) using a Gatan Orius CCD camera and digital micrograph acquisition software (Gatan, Germany). Quantification was performed as described in Yu et al. (Yu et al., 2006).

Primers and plasmids
Primers are listed in Table S3 in the supplementary material. Plasmids are listed in Table 1. If not otherwise stated, 'LazyBoy' plasmids were used as described previously (Neukomm et al., 2011).

RESULTS
A genetic screen for negative regulators of cell corpse clearance in *C. elegans*
In order to identify negative regulators of apoptotic cell corpse clearance, we developed a genetic screen for mutants with increased engulfment activity. The vital dye Acridine Orange (AO) stains internalized apoptotic cells in both *Drosophila melanogaster* and *C. elegans* in vivo (see Fig. S1 in the supplementary material) (Abrams et al., 1993; Gumienny et al., 1999; Kinchen et al., 2008). AO staining was abrogated in engulfment deficient mutants (Fig. 1A,B; see Fig. S1A in the supplementary material). We surmised that a partial restoration of engulfment activity would lead to the reappearance of internalized (thus AO⁺) corpses, which can be observed readily under a fluorescence dissecting microscope. After screening 45,000 haploid genomes, we isolated 13 suppressor mutations that restored AO staining significantly (Fig. 1; see Fig. S1 in the supplementary material), suggesting that they might have restored, at least partially, engulfment activity. Consistent with this hypothesis, all isolated mutants also contained partially reduced numbers of persistent apoptotic cell corpses in 4-fold embryos (see Fig. S1C in the supplementary material). Here, we describe our characterization of one of these suppressors, *op309*.

op309 reduces *ced-6* persistent cell corpse numbers
op309 mutants showed the most pronounced *ced-6* suppressor phenotype, based on the reappearance of AO⁺ germ cell corpses and corpse numbers in 4-fold embryos. We therefore looked in more detail at the kinetics of cell corpse clearance during
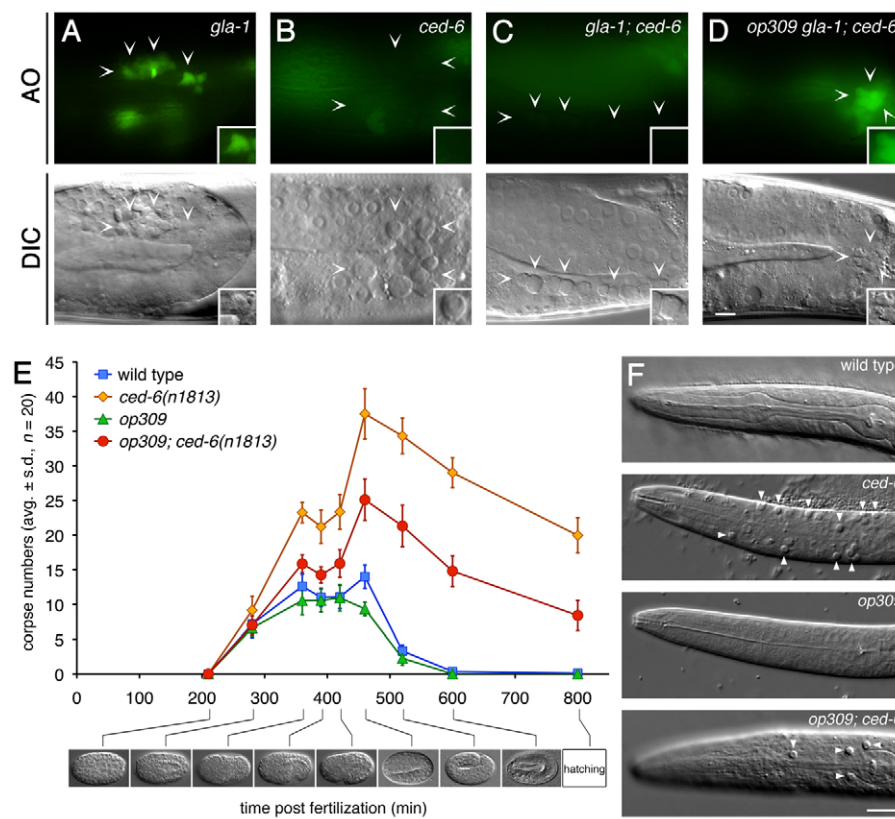
Fig. 1. *op309* reduces the number of persistent apoptotic cell corpses in *C. elegans* engulfment mutants. (**A-D**) *op309* re-allows Acridine Orange (AO) staining (indicative of engulfment) of germ cell corpses in *ced-6* mutants. Staged hermaphrodites of the indicated genotypes were stained 12 hours post-L4/adult molt with AO (green). Open arrowheads indicate clusters of refractive corpses. Higher magnification of representative corpses are shown in insets. Differential interference contrast images are shown below. Anterior is to the left, dorsal on top. Scale bar: 10 µm. (**E**) *op309* reduces the number of embryonic cell corpses. Cell corpses were scored at the following developmental stages: ball of cells (200 minutes post fertilization), tram-track (280 minutes), u-view (360 minutes), bean (385 minutes), 1.5-fold (420 minutes), 2-fold (450 minutes), 3-fold (510 minutes), 4-fold (600 minutes) and hatching (800 minutes). (**F**) *op309* reduces the number of persistent apoptotic cell corpses (arrowheads) in the head of *ced-6* L1 larvae. Scale bar: 10 µm. Alleles used: *gla-1(op234)*, *ced-6(n1813)* and *op309*.

embryonic development. Whereas dying cells were engulfed rapidly in wild-type embryos, removal of cell corpses was delayed in engulfment-deficient *ced-6* animals, resulting in the accumulation of persistent cell corpses in late embryos and freshly hatched L1 larvae (Fig. 1E,F). By contrast, fewer numbers of persistent cell corpses were observed in *op309; ced-6* double mutants at all stages examined, suggesting that *op309* results in reduced persistent cell corpse numbers throughout development.

Apoptosis is not aberrant in *op309* mutants
A reduction in persistent cell corpse numbers could, in principle, be achieved not only through a restoration of engulfment activity but also through reduced apoptosis or a delayed initiation of cell death, as found in *ced-8* mutants (Stanfield and Horvitz, 2000). Whereas ~12 cells remained alive in the anterior pharynx of *ced-3(lf)* mutants, no surviving extra cells were observed in *op309* mutants (Metzstein et al., 1998) (see Fig. S2A in the supplementary material). Furthermore, we observed a normal onset of programmed cell death of the first 12 apoptotic cells in the AB lineage (see Fig. S2B in the supplementary material), as assessed by 4D microscopy (Schnabel et al., 1997; Sulston et al., 1983). We therefore conclude that *op309* does not interfere with developmental apoptosis.

### *ced-6* cell corpse persistence is decreased in *op309* mutants
Next, we asked whether a more efficient cell corpse clearance could explain the reduced *ced-6* persistent cell corpse phenotype in *op309* mutants. Using 4D microscopy, we found that the first 12 cells undergoing apoptosis in wild-type embryos were usually engulfed within 30 minutes upon onset of death (see Fig. S2C and Table S1 in the supplementary material) (Hoeppner et al., 2001; Yu et al., 2006). In *ced-6* mutants, three quarters of the dying cells

(27/36 cells) were engulfed with normal kinetics, whereas the remaining quarter either showed a significant delay in engulfment (3/36 cells) or remained unengulfed until the end of the recording (6/36 cells). Strikingly, *op309; ced-6* double mutants showed nearly wild-type engulfment kinetics, and not a single corpse remained unengulfed. We thus conclude that *op309; ced-6* mutants regained significant engulfment activity, which results in a reduction of persistent cell corpse numbers.

The *op309* mutation could also suppress the internalization defect of apoptotic germ cell corpses in *ced-6* mutants, albeit more weakly than in the soma: *op309; ced-6* double mutants had fewer germ cell corpses than *ced-6* single mutants, and conversely show a partial reappearance of corpses within acidified phagosomes, as measured by AO staining (Fig. 1D; data not shown) and various markers of the phagosome maturation pathway (see Fig. S2D in the supplementary material).

op309 is an allele of the *myotubularin1* gene *mtm-1*
Through a combination of genetic mapping, RNA interference and DNA sequencing, we were able to identify *mtm-1*, the *C. elegans* homolog of human myotubularin 1, as the candidate gene mutated in *op309* mutants. We identified a single point mutation in exon 4 in *op309* mutants (GGA → GAA), which changes a conserved glycine to glutamic acid at codon 106 (G106E) (see Figs S3 and S4 in the supplementary material). There is another *mtm-1* mutant available, *ok742*, which, unlike superficially normal *op309* mutants, arrest development as L2 larvae, suggesting that *mtm-1* function is more strongly impaired in the deletion allele *ok742* than in the point mutant *op309* (Fig. 3A,B). *mtm-1(ok742)* failed to complement the *op309* suppressor phenotype (Fig. 2B), suggesting that *op309* is an allele of *mtm-1*.
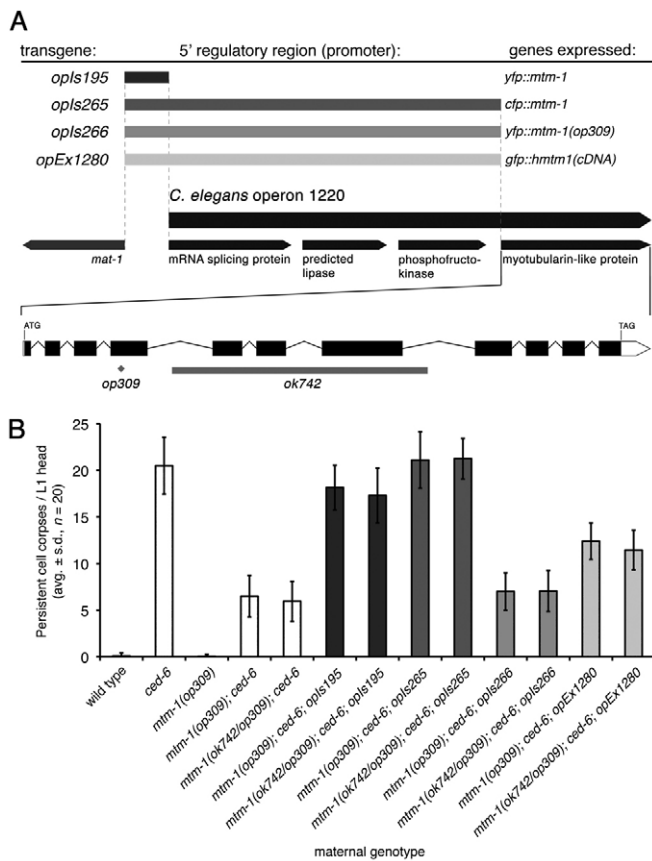
Fig. 2. *mtm-1* rescues the *ced-6* suppressor phenotype of *op309*.
(**A**) *mtm-1* locus and rescue constructs. *mtm-1* is the last gene in the *C. elegans* operon 1220. A short regulatory region (indicated by dashed lines, used in the transgenic line *opIs195*) and a long regulatory region (used in the transgenic lines *opIs265*, *opIs266* and *opEx1280*) were used as promoters. Unless otherwise stated, genomic fragments were used. Color code of the regulatory regions corresponds to the graph in B. Structure of the *mtm-1* locus including alleles is shown below. (**B**) Expression of *mtm-1* rescues the *op309* engulfment phenotype. Hermaphrodites of the indicated genotypes were allowed to self fertilize, and progeny were scored for cell corpses in freshly hatched L1 larval heads. Allele used: *ced-6(n1813)*.

Interestingly, Zou and co-workers independently identified *mtm-1* in an RNAi-screen for suppressors of persistent cell corpses in *ced-1* mutants (Zou et al., 2009). Using our viable *mtm-1(op309)* allele, we confirmed the involvement of MTM-1 as a negative regulator of corpse internalization as shown previously by Zou et al. and expanded further the characterization of *mtm-1* function in *C. elegans*, as described below.

The *C. elegans* genome contains a large number of operons (Blumenthal et al., 2002; Spieth et al., 1993). *mtm-1* is the last member of operon 1220 (CEOP1220), which consists of four genes (Fig. 2A). We expressed *mtm-1(+)* under the control of both a short 'operon promoter' as well as a long 'comprehensive *mtm-1* 5'-regulatory region' which was sufficient to rescue the *mtm-1* engulfment phenotype (Fig. 2B). Importantly, similar constructs driving MTM-1(G106E) failed to rescue, confirming that the G106E substitution impairs normal function of MTM1 and is likely to be the cause of the *op309* phenotype.

The human homolog MTM1 shares 46% identity and 64% similarity with *C. elegans* MTM-1 at the protein level (see Fig. S4 in the supplementary material). To determine whether the molecular function of MTM-1 is conserved through evolution, we expressed hMTM1 under the control of the long *C. elegans mtm-1* promoter (*opEx1280*). hMTM1 efficiently rescued *mtm-1(op309)* mutants, indicating that human myotubularin can substitute functionally for *C. elegans* MTM-1 in the regulation of cell corpse clearance.

MTM-1 is expressed broadly in *C. elegans*

In a previous study, a 1.5 kb *mtm-1* promoter fragment drove MTM-1 expression in a few head and tail neurons (Xue et al., 2003). We re-addressed this question using our rescuing transgenic lines. Both short and long promoters led to a broad expression of MTM-1 in many tissues (see Movie 1 and Fig. S5A-D in the supplementary material). As previously described, we found that MTM-1 is abundantly expressed at the cell cortex (e.g. on the apical membrane of intestinal cells; see Fig. S5D in the supplementary material), with the rest of the protein being distributed throughout the cytosol (Laporte et al., 2002a). The broad expression of MTM-1 and its subcellular localization suggest other functions beside its role in cell corpse clearance, consistent with the lethal phenotype of the deletion allele *mtm-1(ok742)*.

The *op309* mutation reduces MTM-1 phosphoinositide 3-phosphatase activity

mtm-1 belongs to a large and disease-associated family of polyphosphoinositide (PPIn) 3-phosphatases, the myotubularins, which act on phosphatidylinositol-3-phosphate (PtdIns3*P*) and phosphatidylinositol-3,5-diphosphate [PtdIns(3,5)P_2] in mammals (Blondeau et al., 2000; Laporte et al., 2002b; Taylor et al., 2000; Tronchere et al., 2004; Walker et al., 2001). In addition to the phosphatase domain, all myotubularins contain a conserved N-terminal GRAM-PH (glucosyltransferases, Rab-like GTPase activators and myotubularins, pleckstrin-homology) domain, which has been suggested to mediate interaction with PPIn and membranes (Laporte et al., 2001).

Several mammalian members of the myotubularin family contain inactive phosphatase domains (Laporte et al., 2003); we thus asked whether *C. elegans* MTM-1 possesses phosphatase activity. Bacterially expressed *C. elegans* MTM-1 protein readily showed 3-phosphate phosphatase activity towards both PtdIns3*P* and PtdIns(3,5)P_2 in vitro. Interestingly, the phosphatase activity was strongly reduced, but not abrogated in MTM-1(G106E) (Fig. 3C).

To confirm the biochemical activity of MTM-1 in vivo, we visualized levels of one of the MTM-1 PPIn targets, PtdIns3*P*, by a transgenic strain that broadly expresses a fluorescent 2xFYVE domain in vivo (*opIs222[P_{eft-3}::gfp::fyve::fyve]*). Consistent with our in vitro results, *op309* mutants and *mtm-1(RNAi)*-treated animals had significantly higher numbers of PtdIns3*P*-positive vesicles compared with control strains (Fig. 3D,E).

The residual in vitro phosphatase activity of MTM-1(G106E) suggests that *op309* is not a null allele. To test this genetically, we compared the strength of the engulfment defect caused by *op309* and by the deletion allele *ok742*, which completely lacks the phosphatase domain and thus possibly represents a null allele. Interestingly, we did not observe any significant difference between the two *mtm-1* mutations in our assay (Fig. 3F). Taken together, our results suggest that *C. elegans* MTM-1 is a PPIn 3-phosphatase and that *mtm-1(op309)* is a strong reduction-of-function allele with reduced enzymatic activity.
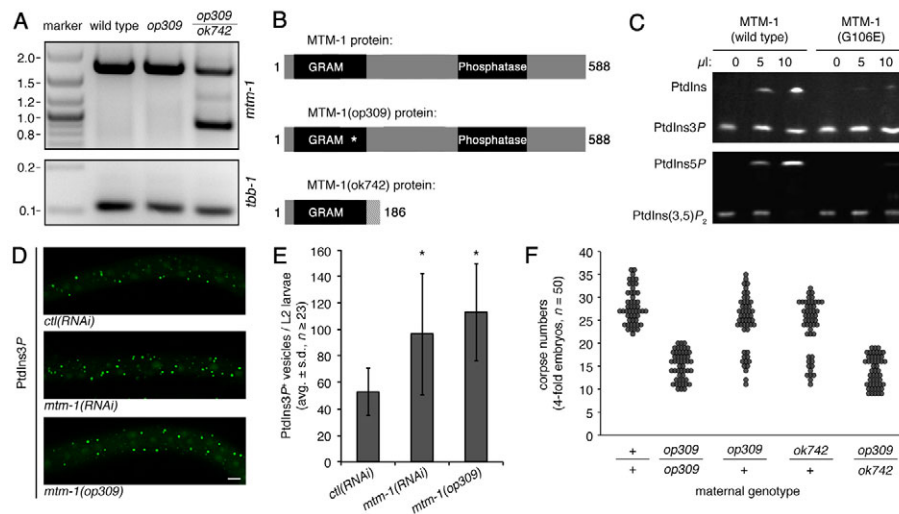
Fig. 3. *mtm-1(op309)* is a reduction-of-function allele. (A) RT-PCR amplification of *mtm-1* from wild-type and mutant total RNA followed by sequencing revealed an 838 nucleotide shortened transcript in *mtm-1(ok742)* mutants. *tbb-1* was used as a control. **(B)** Domain structure of wild-type and mutant MTM-1 proteins. Black boxes, protein domains; white asterisk, G106E mutation; dashed light gray box, 40 out-of-frame amino acids following the *ok742* deletion. **(C)** MTM-1(G106E) shows reduced phosphoinositol 3-phosphate phosphatase activity in vitro. MTM-1 phosphatase activity towards PtdIns3*P* and PtdIns(3,5)P_2 was measured as described in Materials and methods. **(D)** Reduction of *mtm-1* function results in increased PtdIns3*P*-positive (PtdIns3*P*$^+$) vesicles in vivo. Confocal microscopy pictures of hypodermal cells of L2 larvae treated with control RNAi (empty L4440 vector) or *mtm-1(RNAi)*, as well as *mtm-1(op309)* mutants. All animals contain *opIs222[P_{eft-3}::gfp::fyve::fyve]* in the background, a probe that specifically binds PtdIns3*P*. Scale bar: 5 µm. **(E)** Quantification of PtdIns3*P*$^+$ vesicles. Data is shown as number of GFP-positive (2xFYVE) vesicles in hypodermal cells of L2 larvae. *$P<10^{-4}$, determined by *t*-test. **(F)** *mtm-1(op309)* is a reduction-of-function allele in vivo. Hermaphrodites of the indicated genotypes were allowed to self fertilize, and cell corpses were scored in their 4-fold embryo progeny. Each dot represents a single embryo (*n*=50). All strains were homozygous for the *ced-6(n1813)* mutation. Alleles used: *mtm-1(ok742/op309)* and *ced-6(n1813)*.

The results above are surprising insofar as the *op309* mutation does not affect the catalytic phosphatase domain, but rather a residue in the GRAM-PH domain. We surmise that the G106E mutation alters the overall conformation of MTM-1 or the oligomerization that was shown to be important for allosteric activation (Schaletzky et al., 2003) and thereby interferes with the enzymatic activity.

mtm-1 is the major engulfment regulator among myotubularin family members

The myotubularin family is grouped into six subfamilies, based on catalytic activity as well as domain content. Each subfamily is represented by a single gene in *C. elegans*: *mtm-1*, *mtm-3*, *mtm-5*, *mtm-6*, *mtm-9* and *mtm-12* (Laporte et al., 2003). To determine whether other myotubularin family members might also be involved in the regulation of cell corpse clearance, we tested existing mutants (or RNAi-treated animals) for their ability to suppress *ced-6* mutants. MTM-1 was the only family member able to dramatically suppress apoptotic cell corpse persistence (see Fig. S6 in the supplementary material). Thus, we conclude that *mtm-1* is likely to be the major myotubularin involved in the regulation of cell corpse clearance.

mtm-1 acts upstream of *ced-2*, *ced-5* and *ced-12*

To determine where *mtm-1* acts within the engulfment signaling pathway, we performed an in depth set of double and triple mutant analysis. Both the viable *mtm-1(op309)* and the lethal *mtm-1(ok742)* mutations were able to suppress loss-of-function alleles of *ced-1*, *ced-6* and *ced-7* (Table 2A), suggesting that *mtm-1* acts downstream or in parallel to the *ced-1*, *ced-6* and *ced-7* pathway.

By contrast, *mtm-1* was unable to suppress the engulfment defect of mutations in *ced-2*, *ced-5* and *ced-12* mutant worms, three genes that act in a signaling pathway in parallel to *ced-1*, *ced-6* and *ced-7* (Table 2B). These findings suggest that MTM-1 functions in this pathway, probably upstream of *ced-2*, *ced-5* and *ced-12*.

mtm-1 was also able to suppress two different hypomorphic *ced-10* alleles: *n1993*, a mutation in the C-terminal CAAX prenylation motif (affecting localization rather than function), and *n3246* (impaired nucleotide binding). However, this *ced-10* suppression was *ced-5* dependent (*ced-10 ced-5* versus *mtm-1; ced-10 ced-5*), indicating that *mtm-1* suppression of *ced-10* mutants requires *ced-5* function (and that these two mutant proteins can be activated by CED-5 to some degree). Taken together, our results clearly suggest that *mtm-1* acts in parallel to *ced-7*, *ced-1* and *ced-6*, and upstream of the ternary *ced-2–ced-5–ced12* GEF complex, which in turn modulates *ced-10* activity.

mtm-1 acts in parallel to *mig-2*

We next tested whether *mtm-1* might function at the same step as the GTPase *mig-2*, which is known to act as a positive regulator of CED-12 (deBakker et al., 2004). *mig-2(mu28)*, an early stop allele, did not revert the *ced-6* suppressor phenotype of *mtm-1* (Table 3), suggesting that *mtm-1* acts downstream or in parallel to *mig-2*.

We also analyzed the rare gain-of-function allele *mig-2(gm103gf)*, which is equivalent to transforming mutations in codon 12 of Ras. The MIG-2(G16E) mutation prevents GTP hydrolysis and thus renders the protein constitutively active (Forrester and Garriga, 1997; Zipkin et al., 1997). We surmised that this mutation, by constitutively activating the CED-5–CED-12 GEF complex, should, like *mtm-1(op309)*, be able to partially compensate for defects in the *ced-1/ced-6/ced-7* signaling pathway.

Table 2. mtm-1 acts downstream of or in parallel to the *ced-7*, *ced-1*, *ced-6* and *dyn-1* signaling pathway, but acts upstream of *ced-2*, *ced-12* and *ced-5*

Genotype	Refractive corpses (mean ± s.d., n=20)*
(A) *mtm-1* acts downstream of or in parallel to *ced-1*, *ced-6* and *ced-7*	
wild type	0.1±0.2
mtm-1(ok742)	0.0±0.0
mtm-1(op309)	0.0±0.0
ced-1(e1735)	21.6±2.7
mtm-1(ok742) ced-1(e1735)	9.3±2.5
mtm-1(op309) ced-1(e1735)	10.0±2.9
ced-1(n1995)	6.9±2.5
mtm-1(op309) ced-1(n1995)	3.9±1.7
ced-6(n1813)	21.5±2.2
mtm-1(ok742); ced-6(n1813)	8.3±2.6
mtm-1(op309); ced-6(n1813)	6.4±2.4
ced-6(tm1826)	24.3±2.1
mtm-1(op309); ced-6(tm1826)	9.1±2.6
ced-6(op360)	10.4±2.3
mtm-1(op309); ced-6(op360)	6.0±2.2
ced-7(n1996)	21.1±2.5
mtm-1(ok742); ced-7(n1996)	n.d.
mtm-1(op309); ced-7(n1996)	6.2±2.6
ced-7(n1892)	21.9±2.2
mtm-1(op309); ced-7(n1892)	14.6±2.4
ced-7(n2690)	21.4±3.2
mtm-1(op309); ced-7(n2690)	9.1±2.5
dyn-1(n4039)	20.1±1.3†
mtm-1(op309); dyn-1(n4039)	14.3±3.3†
(B) *mtm-1* acts upstream of *ced-2*, *ced-5* and *ced-12*	
ced-2(n1994)	17.2±3.5
mtm-1(ok742); ced-2(n1994)	18.1±1.9
mtm-1(op309); ced-2(n1994)	17.0±3.3
ced-2(e1752)	15.6±2.6
mtm-1(op309); ced-2(e1752)	13.4±2.9
ced-5(n1812)	22.7±2.5
mtm-1(ok742); ced-5(n1812)	21.4±2.9
mtm-1(op309); ced-5(n1812)	22.5±2.2
ced-5(n2002)	22.1±2.9
mtm-1(op309); ced-5(n2002)	22.3±2.7
ced-5(tm1949)	24.1±2.0
mtm-1(op309); ced-5(tm1949)	24.3±2.2
ced-12(k149)	20.3±1.9
mtm-1(ok742) ced-12(k149)	19.1±2.6
mtm-1(op309) ced-12(k149)	18.7±2.7
ced-12(bz187)	18.9±2.7
mtm-1(op309) ced-12(bz187)	18.1±2.4
ced-12(oz167)	18.5±3.2
mtm-1(op309) ced-12(oz167)	15.1±3.3
ced-10(n1993)	15.8±1.9
mtm-1(ok742); ced-10(n1993)	7.1±2.1
mtm-1(op309); ced-10(n1993)	5.6±2.3
ced-10(n3246)	20.8±2.6
mtm-1(op309); ced-10(n3246)	10.0±3.0
ced-10(n3246) ced-5(n1812)	19.6±1.7
mtm-1(op309); ced-10(n3246) ced-5(n1812)	19.5±2.0

*Cell corpses were scored in L1 larval heads of the indicated genotypes.
†Corpse numbers of early 4-fold embryos as *dyn-1(n4039)* embryos fail to hatch.
n.d., not determined.

Table 3. *mtm-1* acts in parallel to *mig-2*

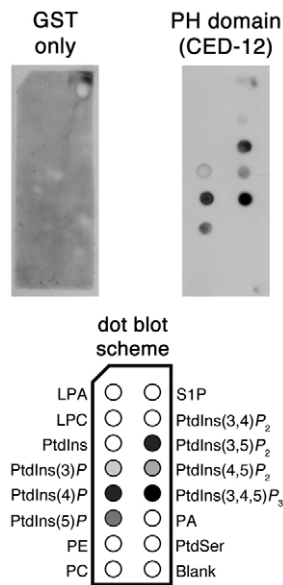| Genotype	Refractive corpses (mean ± s.d., n=20)*
wild type	0.2±0.2
mig-2(mu28)	0.2±0.5
mtm-1(op309)	0.0±0.0
mtm-1(op309); mig-2(mu28)	0.0±0.0
ced-6(n1813)	21.5±2.2
ced-6(n1813); mig-2(mu28)	21.5±2.2
mtm-1(op309); ced-6(n1813)	6.9±2.4
mtm-1(op309); ced-6(n1813); mig-2(mu28)	10.1±3.1
mig-2(gm103gf)	0.0±0.0
mtm-1(op309); mig-2(gm103gf)	0.0±0.0
ced-6(n1813)	21.5±2.2
ced-6(n1813); mig-2(gm103gf)	6.4±2.0
mtm-1(op309); ced-6(n1813)	6.9±2.4
mtm-1(op309); ced-6(n1813); mig-2(gm103gf)	0.9±0.9
ced-1(e1735)	21.6±2.7
ced-1(e1735); mig-2(gm103gf)	11.6±2.7
mtm-1(op309) ced-1(e1735)	10.0±2.9
mtm-1(op309) ced-1(e1735); mig-2(gm103gf)	6.9±1.9
ced-7(n1996)	21.1±2.5
ced-7(n1996); mig-2(gm103gf)	6.4±2.2
mtm-1(op309); ced-7(n1996)	6.2±2.6
mtm-1(op309); ced-7(n1996); mig-2(gm103gf)	3.9±1.5
ced-2(n1994)	17.2±3.5
ced-2(n1994); mig-2(gm103gf)	1.2±1.1
mtm-1(op309); ced-2(n1994)	17.0±3.3
mtm-1(op309); ced-2(n1994); mig-2(gm103gf)	1.4±1.1
ced-5(n1812)	22.7±2.5
ced-5(n1812); mig-2(gm103gf)	22.5±2.5
mtm-1(op309); ced-5(n1812)	22.5±2.2
mtm-1(op309); ced-5(n1812); mig-2(gm103gf)	22.9±2.0
ced-12(k149)	20.3±1.9
ced-12(k149); mig-2(gm103gf)	20.7±2.9
mtm-1(op309) ced-12(k149)	18.7±2.7
mtm-1(op309) ced-12(k149); mig-2(gm103gf)	20.4±2.3
ced-10(n1993)	15.8±1.9
ced-10(n1993); mig-2(gm103gf)	5.6±1.7
mtm-1(op309); ced-10(n1993)	5.6±2.3
mtm-1(op309); ced-10(n1993); mig-2(gm103gf)	2.5±0.9

*Cell corpses were scored in the L1 larval heads of the indicated genotypes. Some scores are used from Table 2.

observed in *ced-1*, *ced-6* and *ced-7* mutant worms. Consistent with its proposed role as a regulator of the bipartite CED-5–CED-12 GEF complex, *mig-2(gm103gf)* could not suppress *ced-5* and *ced-12* mutants. By contrast, *mig-2(gf)* effectively suppressed *ced-2* mutants, suggesting that MIG-2 regulates CED-5–CED-12 in a CED-2-independent manner.

Taken together, our results suggest that MIG-2 and MTM-1 act in parallel to each other, one as a positive and the other as a negative regulator of the CED-5–CED-12 GEF complex. Moreover, the differential response of *ced-2* mutants to *mig-2* and *mtm-1* suggest that these two proteins influence CED-5–CED-12 via different molecular processes (Fig. 6A).

The membrane-binding domains of the CED-5–CED-12 GEF complex bind PtdIns(3,5)*P₂* in vitro

How does MTM-1 regulate the CED-5–CED-12 GEF complex? PPIn have been implicated in the recruitment and activation of GEFs and GAPs (Saarikangas et al., 2010). As MTM-1 contains 3-phosphate phosphatase activity towards at least two different PPIn, it is tempting to speculate that MTM-1 influences engulfment signaling by modulating plasma membrane PPIn levels and

Consistent with this hypothesis, the *mig-2(gm103gf)* mutation strongly suppressed the engulfment defect of *ced-1*, *ced-6* and *ced-7* mutants (Table 3).

Strikingly, we observed that loss of *mtm-1* function and gain of *mig-2* function could cooperate to generate an even stronger suppression of engulfment defects. This additive effect was

Fig. 4. The PH domain of CED-12 mainly binds PtdIns(3,5)P_2, PtdIns4P and PtdIns(3,4,5)P_3 in vitro. GST::PH(CED-12) and GST alone were tested for lipid-binding ability on dot blots. A schematic dot blot below indicates affinities towards particular lipids. Black, dark gray, medium gray, light gray and white represent relative binding strengths (from strong binding to no binding at all). LPA, lysophosphatidic acid; LPC, lysophosphatidylcholine; PtdIns, phosphatidylinositol; PE, phosphatidylethanolamine; PC, phosphatidylcholine; S1P, sphingosine-1-phosphate; PA, phosphatidylalanine; PtdSer, phosphatidylserine.

subsequently CED-5–CED-12 recruitment. Consistent with this hypothesis, previous work has shown that Dock180, the mammalian homolog of CED-5, contains a phospholipid binding domain (DHR1), which interacts in vitro with PtdIns(3,5)P_2 and PtdIns(3,4,5)P_3 and mediates membrane translocation of the Dock180/ELMO GEF complex (Côté et al., 2005). However, we could not detect interaction between the CED-5 DHR1 domain and any phospholipid in vitro (data not shown).

CED-12 contains a pleckstrin homology (PH) domain which is required for the GEF function with CED-5 (Zhou et al., 2001a). Many PH domains have been shown to bind to PPIn (Lemmon, 2008), suggesting that the CED-12 PH domain might also contribute to GEF recruitment to the plasma membrane. To test this hypothesis directly, we cloned and expressed a GST CED-12 PH domain fusion (GST::PH$_{CED-12}$), and measured its lipid binding ability and specificity on dot blots (Fig. 4), where PtdIns4P, PtdIns(3,5)P_2 and PtdIns(3,4,5)P_3 were strongly bound by PH$_{CED-12}$.

These observations led us to speculate that the PH domain of CED-12 might not only stabilize the nucleotide free CED-5–CED-10 complex (Ravichandran and Lorenz, 2007), but probably also contributes to the phosphoinositide-dependent recruitment or activation of the CED-5–CED-12 GEF complex at phagocytic cups.

MTM-1 knockdown results in persistent but engulfed cell corpses in the somatic germline

We originally focused on *mtm-1* as the candidate gene mutated in *op309* because *mtm-1(RNAi)*, like the *op309* mutation, can suppress the internalization defect of *ced-6* mutants, and thereby lead to a reappearance of internalized (or AO$^+$) germ cell corpses

in the adult germline (see above). Surprisingly, as part of a control experiment, we noticed that knockdown of *mtm-1* in wild-type animals can, by itself, also interfere with cell corpse clearance, as *mtm-1(RNAi)* animals often showed increased numbers of germ cell corpses compared with control strains (Fig. 5A). Importantly, we observed this phenotype in three independent *mtm-1(RNAi)* clones (see Fig. S7 in the supplementary material), which argues against (but does not exclude) an off-target effect as a cause of this additional germ cell corpse phenotype (Rual et al., 2007).

To determine whether these germ cell corpses are not engulfed, or are engulfed but not degraded, we analyzed the gonads of staged *mtm-1(RNAi)*-treated adult hermaphrodites using transmission electron microscopy (TEM) (Fig. 5B,C). In wild-type gonads, apoptotic germ cells pinch off the germline syncytium and are rapidly internalized and degraded by the surrounding somatic sheath cells (Gumienny et al., 1999). In *ced-1; ced-5* double mutant animals, which are defective in cell corpse recognition and internalization, apoptotic cells accumulate as uninternalized corpses between the syncytial germline and the surrounding sheath cells (Fig. 5C). By contrast, all cell corpses observed in *mtm-1(RNAi)* animals were readily internalized and found within sheath cell phagosomes.

gla-3 and *gla-1* function in the hermaphrodite germline (Kritikou et al., 2006; Lettre et al., 2004). Loss of gla gene function superficially results in a similar germ cell corpse phenotype as observed in *mtm-1(RNAi)* treated animals: in *gla-3* mutants, all germ cell corpse observed localized inside sheath cells (Fig. 5C). To determine whether the increase in internalized germ cell corpses observed in *mtm-1(RNAi)* is due to either increased germ cell apoptosis or reduced degradation in the somatic gonad, we measured germ cell corpse numbers in animals defective for cell corpse internalization. Whereas *gla-1; ced-6* double mutants had significantly more germ cell corpses than either single mutant (many cells died, none could be engulfed), germ cell corpse number in *mtm-1(RNAi); ced-6* animals was not increased compared with *mtm-1(RNAi)* alone (see Table S2 in the supplementary material). We therefore concluded that germ cell apoptosis is not affected, but rather that germ cell corpses fail to be properly degraded in *mtm-1(RNAi)* treated animals.

To decipher whether the germ cell corpse degradation defect observed in *mtm-1(RNAi)* animals is due to a loss of MTM-1 function in the dying or the engulfing cell, we repeated the RNAi-mediated *mtm-1* knockdown in two specific mutant backgrounds: *rrf-1(pk1417)*, which are defective in somatic RNAi; and *mut-7(pk204)*, in which germline RNAi is abrogated (Ketting et al., 1999; Sijen et al., 2001). As expected, *gla-1(RNAi)* and *ced-3(RNAi)* were still effective in somatic RNAi-deficient *rrf-1* mutants, but failed to induce any change in the germline-defective *mut-7* background. By contrast, *mtm-1(RNAi)* resulted in increased germ cell corpse numbers only in germline-defective *mut-7* animals, implying that *mtm-1* function is required in the soma, probably in the gonadal sheaths cells, for effective germ cell corpse degradation.

The results above indicate that *mtm-1(RNAi)* reduces cell corpse clearance at a stage post corpse internalization. To determine at which stage *mtm-1* acts during phagosome maturation, we applied RNAi-mediated knockdown of *gla-1* and *mtm-1* and compared the recruitment of various fluorescent phagosome maturation reporters (Kinchen et al., 2008; Nieto et al., 2010; Yu, 2008) (see Fig. S8 in the supplementary material). Interestingly, many more phagosomes in *mtm-1(RNAi)*-treated animals still contained high levels of CED-1, compared with control strains. However, because late-stage markers still efficiently labeled corpses in *mtm-1(RNAi)* animals,
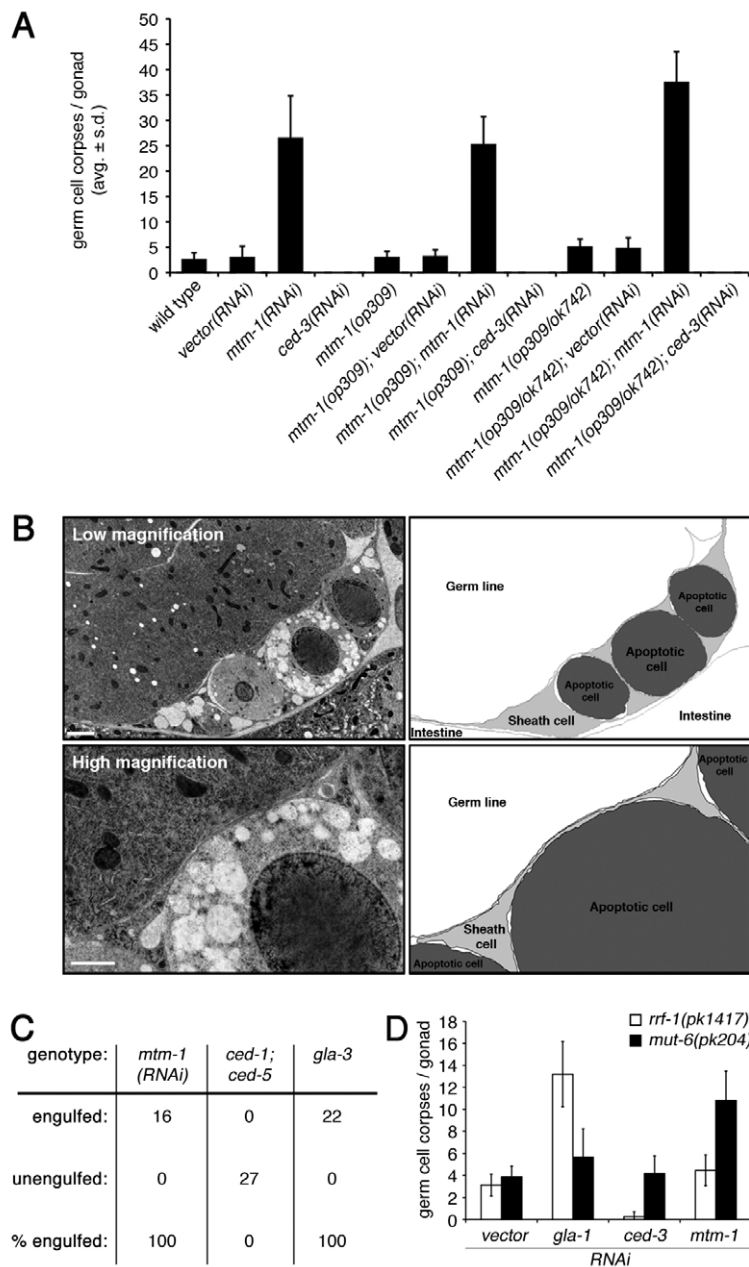
Fig. 5. *mtm-1* knockdown results in engulfed but persistent germ cell corpses. (**A**) *mtm-1(RNAi)* results in increased germ cell corpse numbers. Indicated genotypes were grown on corresponding bacterial RNA interference clones. Staged hermaphrodites were scored 12 hours post-L4/adult molt. Scores: three independent experiments (*n*=20 for each experiment). (**B**) *mtm-1(RNAi)* results in the accumulation of engulfed but undegraded germ cell corpses. Transmission electron microscopy (TEM) images of cell corpses and their neighboring cells, and corresponding camera lucida drawings. Representative low (top) and high (bottom) magnification examples are shown on the left, corresponding schemes on the right. Apoptotic cells are represented in dark gray, sheath cells in light gray and the germline syncytium in white. Staged *mtm-1(RNAi)*-treated hermaphrodites (12 hours post-L4/adult molt) were prepared for TEM analysis as described in Materials and methods. Scale bars: 2 μm for low magnification; 1 μm for high magnification. (**C**) TEM germ cell corpse number quantification. Corpses were scored as described in Materials and methods and by Yu et al. (Yu et al., 2006). Alleles used: *ced-1(e1735)*, *ced-5(n1812)* and *gla-3(op216)*. (**D**) *mtm-1* functions in the engulfing sheath cells. *rrf-1* is required for somatic and *mut-7* for germline RNA interference (Ketting et al., 1999; Sijen et al., 2001). Knockdown of *mtm-1* in the soma results in persistent (but engulfed) germ cell corpse phenotype. Staged hermaphrodites were scored 12 hours post-L4/adult molt. Data shown are mean ± s.d., *n*=20 scores for each of three independent experiments.

we conclude that loss of *mtm-1* does not generally block phagosome maturation, but rather might interfere, directly or indirectly, with CED-1 receptor recycling.

Our findings suggest that MTM-1 is required at least twice during the process of cell corpse clearance. First, MTM-1 negatively regulates cell corpse recognition and internalization, probably by limiting recruitment or activation of the CED-5–CED-12 GEF complex at the phagocytic cup. Following internalization, MTM-1 function is required once more, this time to promote, directly or indirectly, recycling of the CED-1 receptor.

Increased engulfment activity can kill cells close to death

Loss of engulfment activity, besides leading to corpse persistence, also promotes cell survival (Hoeppner et al., 2001; Reddien et al., 2001). Conversely, increased engulfment activity leads to reduced sick cell survival (Neukomm et al., 2011). We thus determined whether loss of *mtm-1* function can also lead to increased elimination of cells on the verge of death, by scoring P*n*.aap cell survival in weak *ced-3* reduction-of-function (rf) mutants showing limited caspase activity (see Fig. S9A in the supplementary material). Loss of *mtm-1* function reduced survival of the supernumerary P*n*.aap cells by ~50% in *ced-3(rf)* mutants (see Fig. S9B in the supplementary material). Importantly, this increased killing activity was dependent on a functional engulfment machinery, as loss of *mtm-1* had no effect in either *ced-5* or *ced-6* mutant animals. Our results demonstrate that loss of *mtm-1* function, probably by over-activation of the engulfment signaling cascade(s), can promote the removal of cells that are viable but fated to die.

DISCUSSION

Here, we described our identification and characterization of *mtm-1*, a PPIn phosphatase that acts at multiple steps to regulate apoptotic cell clearance in *C. elegans*. First, consistent with results

from Zou and colleagues (Zou et al., 2009), who independently identified *mtm-1* as a negative regulator of corpse internalization in an RNAi screen, we found that loss of *mtm-1* partially restores phagocytic activity in mutants defective in corpse recognition and internalization. Epistatic analyses indicated that MTM-1 controls internalization by negatively regulating the CED-5–CED-12 GEF complex together with CED-2, which promotes GTP-loading of the CED-10 GTPase. Zou et al. described a *ced-2* suppression by *mtm-1*. We did not observe such a suppression in our assay, which could be explained by the different developmental stages used for epistatic analyses (4-fold embryos versus L1 heads, respectively). Expression of human MTM1 partially rescued *mtm-1* mutants, suggesting a conserved molecular function for this gene in the regulation of Rac1-dependent cytoskeletal rearrangements. Second, we showed that loss of *mtm-1* leads to the accumulation of internalized but undegraded cell corpses. Our observations suggested that MTM-1 is required for proper maturation of phagosomes containing apoptotic corpses, in particular for the recycling of the apoptotic cell corpse receptor CED-1.

Biochemical analysis of the mutant protein revealed that MTM-1, like its mammalian ortholog, has phosphoinositide 3-phosphatase activity towards PtdIns$3P$ and PtdIns$(3,5)P_2$ in vitro. Interestingly, CED-5 and CED-12, the two subunits of the CED-10 GEF complex, can both bind PtdIns$(3,5)P_2$.

PtdIns$(3,5)P_2$ is a low abundance PPIn, commonly present at 0.1% or less of total cellular PPIn (Michell et al., 2006). However, PtdIns$(3,5)P_2$ is present in all eukaryotic cells so far examined and thus presumably contributes to widely conserved cell function(s). Surprisingly, the membrane binding domain of CED-5, DHR1, binds with approximately the same affinity to PtdIns$(3,4,5)P_3$ and to PtdIns$(3,5)P_2$ in vitro (Côté et al., 2005). We similarly found that the PH membrane-binding domain of CED-12 also binds to PtdIns$(3,5)P_2$ in vitro. It is thus tempting to propose that recruitment or activation of the CED-5–CED-12 GEF complex might be mediated through binding to PtdIns$(3,5)P_2$ generated on the inner leaflet of the phagocytic cup. Through hydrolysis of PtdIns$(3,5)P_2$ to PtdIns$5P$, MTM-1 would antagonize GEF recruitment and/or activation, possibly as part of a negative feedback loop (Fig. 6B). Consistent with this hypothesis, overexpression of dominant active Rac1 in mammalian cells recruits hMTM1 to Rac1-induced membrane ruffles, where hMTM1 might dephosphorylate PtdIns$(3,5)P_2$, thereby blocking further GEF complex recruitment (Laporte et al., 2002a). As we failed to detect any enrichment of a functional CED-12::GFP reporter around phagocytic cups or early internalized corpses in the adult gonad (data not shown), we suspect that localized activation, rather than physical recruitment, might be the major mode of CED-5–CED-12 regulation by PPIn. Alternatively, CED-5–CED-12 association with the phagocytic cup might simply be too transient to be detected by this method.

Our analysis of an MTM-1 reporter construct revealed a broad MTM-1 expression in *C. elegans*. We found that the protein is often abundant at the plasma membrane, consistent with the model presented above. However, we also observed significant amounts of MTM-1 in the cytosol, suggesting that the protein might also be acting on other cellular membranes. Indeed, PtdIns$3P$ and PtdIns$(3,5)P_2$, the two known substrates for MTM-1, are present on the surface of various intermediates of the endosomal pathway (Robinson and Dixon, 2006). Evidence that MTM-1 also hydrolyzes PPIn in the endosomal pathway is provided by the increase in PtdIns$3P$-positive vesicles in hypodermal cells of *mtm-1(op309)* and *mtm-1(RNAi)* animals.
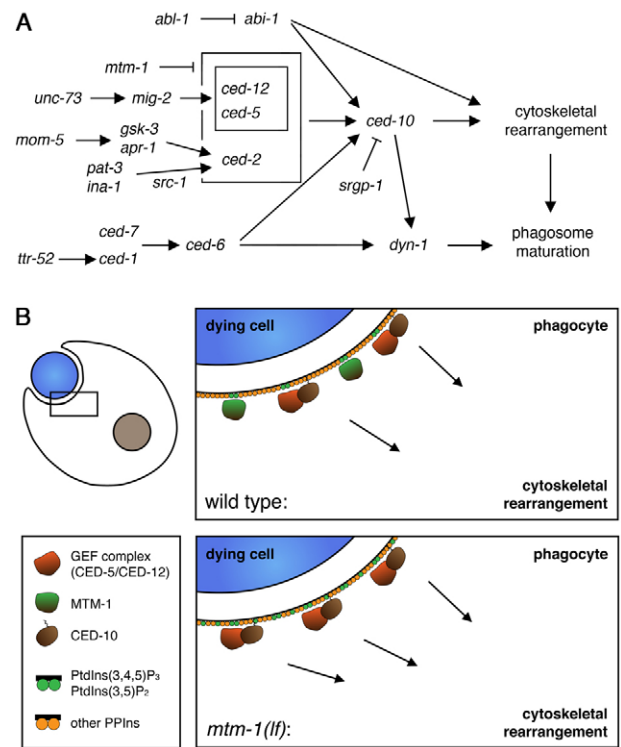
Fig. 6. Model of MTM-1 function in cell corpse clearance in *C. elegans*. (**A**) Genetic pathways for apoptotic cell corpse clearance. Three 'parallel' pathways contribute to cell corpse clearance in *C. elegans*. *abl-1* and *abi-1* act in a first pathway, *mom-5*, *gsk-3*, *apr-1*, *ina-1*, *pat-3*, *src-1*, *unc-73*, *mig-2*, *mtm-1*, *ced-2*, *ced-5* and *ced-12* in a second, and *ttr-52*, *ced-7*, *ced-1*, *ced-6* and *dyn-1* in a third pathway. All pathways probably converge at the level of *ced-10*, which is negatively regulated by *srgp-1*. *ced-10* orchestrates cytoskeletal rearrangements around the cell corpse, followed by corpse internalization and phagosome maturation. The *ced-7*, *ced-1* and *ced-6* pathway might also activate the phagosome maturation pathway via *dyn-1*. Components required for phagosome maturation and cell corpse degradation are not shown. (**B**) MTM-1 regulation of engulfment signaling. In wild-type animals, upon cell corpse recognition the CED-5–CED-12 GEF complex is recruited to the inner leaflet of the plasma membrane in phagocytes. Major polyphosphoinositide (PPIn) targets of the GEF complex are PtdIns$(3,4,5)P_3$ and/or PtdIns$(3,5)P_2$. PPIn-bound GEF complex activates the small GTPase CED-10, which leads to cytoskeletal rearrangements. MTM-1 dephosphorylates such PPIn, thus regulating cell corpse clearance through GEF complex plasma membrane recruitment. Loss of MTM-1 function will result in the accumulation of PPIn, which serve as GEF targets at the plasma membrane. As a result, more GEF complexes are recruited to the plasma membrane, which eventually leads to increased CED-10 signaling. The potential function of *mtm-1* within the phagosome maturation process is not shown.

In addition to promoting internalization, we found that knockdown of *mtm-1* interfered with phagosome maturation, leading to the accumulation of internalized, but undegraded apoptotic germ cell corpses within phagosomes of the engulfing sheath cell. Consistent with previous observations, not only phosphorylation, but also dephosphorylation, of PPIn by PPIn phosphatases is required for the proper maturation of endosomes and phagosomes, e.g. via the phosphoinositide 3-kinase VPS-34 (Cremona et al., 1999; Kinchen et al., 2008; Zou et al., 2009).

However, as we could detect phagosomes at all stages of maturation, loss of *mtm-1* is unlikely to block maturation at a specific step. Rather, we suggest, based on the increase in CED-1-positive phagosomes in *mtm-1(RNAi)* animals, that MTM-1 is required for efficient recycling of CED-1 from the phagosome back to the plasma membrane. Interestingly, loss-of-function mutations in *snx-1* and *snx-6*, two PX-domain containing subunits of the *C. elegans* retromer complex, led to a similar defect in germ cell corpse degradation and the accumulation of internalized, CED-1-positive phagosomes (Chen et al., 2010). Whether MTM-1 and the retromer complex, which is known to bind to PPIn, act in the same molecular pathway remains to be determined.

Intriguingly, we did not observe any persistence of embryonic cell deaths in *mtm-1(RNAi)* animals. There are several possible explanations for this observation, ranging from differences in RNAi sensitivity to differential requirements for MTM-1 in phagosome maturation. For example, whereas embryonic cells rarely need to engulf more than one apoptotic cell, the gonadal sheath cells take up and degrade several hundred apoptotic germ cells over the adult life of the animal (Gumienny et al., 1999; Sulston et al., 1983). It is thus possible that the phagosome maturation pathway in sheath cells is more sensitive to interference. Consistent with this hypothesis, animals treated with *vps-34(RNAi)*, in which persistent cell corpses are readily observed in the germline, but fail to be observed in early embryos (Kinchen et al., 2008) (our unpublished results), present experimental evidence for increased RNAi susceptibility in sheath cells compared with the soma.

The myotubularin family of PPIn 3-phosphatases, which dephosphorylate PtdIns3P and PtdIns$(3,5)P_2$), are associated with a variety of human syndromes (such as peripheral Charcot-Marie-Tooth (CMT) neuropathies with or without associated glaucoma, myotubular myopathy) as well as impaired spermatogenensis and azoospermia in mice (Azzedine et al., 2003; Bolino et al., 2000; Firestein et al., 2002; Houlden et al., 2001; Laporte et al., 2003; Nicot and Laporte, 2008; Senderek et al., 2003). However, the molecular mechanisms causing these phenotypes are not understood. As each myotubularin subfamily is represented by a single member in *C. elegans*, further study of myotubularin function in nematodes might shed new light into the cellular and molecular roles of this important family of proteins.

Competing interests statement
The authors declare no competing financial interests.

Supplementary material
Supplementary material for this article is available at http://dev.biologists.org/lookup/suppl/doi:10.1242/dev.060012/-/DC1

References
Abrams, J. M., White, K., Fessler, L. I. and Steller, H. (1993). Programmed cell death during Drosophila embryogenesis. *Development* 117, 29-43.

Akakura, S., Kar, B., Singh, S., Cho, L., Tibrewal, N., Sanokawa-Akakura, R., Reichman, C., Ravichandran, K. S. and Birge, R. B. (2005). C-terminal SH3 domain of CrkII regulates the assembly and function of the DOCK180/ELMO Rac-GEF. *J. Cell. Physiol.* 204, 344-351.

Azzedine, H., Bolino, A., Taieb, T., Birouk, N., Di Duca, M., Bouhouche, A., Benamou, S., Mrabet, A., Hammadouche, T., Chkili, T. et al. (2003). Mutations in MTMR13, a new pseudophosphatase homologue of MTMR2 and Sbf1, in two families with an autosomal recessive demyelinating form of Charcot-Marie-Tooth disease associated with early-onset glaucoma. *Am. J. Hum. Genet.* 72, 1141-1153.

Blondeau, F., Laporte, J., Bodin, S., Superti-Furga, G., Payrastre, B. and Mandel, J. L. (2000). Myotubularin, a phosphatase deficient in myotubular myopathy, acts on phosphatidylinositol 3-kinase and phosphatidylinositol 3-phosphate pathway. *Hum. Mol. Genet.* 9, 2223-2229.

Blumenthal, T., Evans, D., Link, C. D., Guffanti, A., Lawson, D., Thierry-Mieg, J., Thierry-Mieg, D., Chiu, W. L., Duke, K., Kiraly, M. et al. (2002). A global analysis of Caenorhabditis elegans operons. *Nature* 417, 851-854.

Bolino, A., Muglia, M., Conforti, F. L., LeGuern, E., Salih, M. A., Georgiou, D. M., Christodoulou, K., Hausmanowa-Petrusewicz, I., Mandich, P., Schenone, A. et al. (2000). Charcot-Marie-Tooth type 4B is caused by mutations in the gene encoding myotubularin-related protein-2. *Nat. Genet.* 25, 17-19.

Brenner, S. (1974). The genetics of Caenorhabditis elegans. *Genetics* 77, 71-94.

Cabello, J., Neukomm, L. J., Gunesdogan, U., Burkart, K., Charette, S. J., Lochnit, G., Hengartner, M. O. and Schnabel, R. (2010). The Wnt pathway controls cell death engulfment, spindle orientation, and migration through CED-10/Rac. *PLoS Biol.* 8, e1000297.

Chen, D., Xiao, H., Zhang, K., Wang, B., Gao, Z., Jian, Y., Qi, X., Sun, J., Miao, L. and Yang, C. (2010). Retromer is required for apoptotic cell clearance by phagocytic receptor recycling. *Science* 327, 1261-1264.

Côté, J. F., Motoyama, A. B., Bush, J. A. and Vuori, K. (2005). A novel and evolutionarily conserved PtdIns(3,4,5)P3-binding domain is necessary for DOCK180 signalling. *Nat. Cell Biol.* 7, 797-807.

Cremona, O., Di Paolo, G., Wenk, M. R., Luthi, A., Kim, W. T., Takei, K., Daniell, L., Nemoto, Y., Shears, S. B., Flavell, R. A. et al. (1999). Essential role of phosphoinositide metabolism in synaptic vesicle recycling. *Cell* 99, 179-188.

De Stasio, E. A. and Dorman, S. (2001). Optimization of ENU mutagenesis of Caenorhabditis elegans. *Mutat. Res.* 495, 81-88.

deBakker, C. D., Haney, L. B., Kinchen, J. M., Grimsley, C., Lu, M., Klingele, D., Hsu, P. K., Chou, B. K., Cheng, L. C., Blangy, A. et al. (2004). Phagocytosis of apoptotic cells is regulated by a UNC-73/TRIO-MIG-2/RhoG signaling module and armadillo repeats of CED-12/ELMO. *Curr. Biol.* 14, 2208-2216.

Firestein, R., Nagy, P. L., Daly, M., Huie, P., Conti, M. and Cleary, M. L. (2002). Male infertility, impaired spermatogenesis, and azoospermia in mice deficient for the pseudophosphatase Sbf1. *J. Clin. Invest.* 109, 1165-1172.

Forrester, W. C. and Garriga, G. (1997). Genes necessary for C. elegans cell and growth cone migrations. *Development* 124, 1831-1843.

Fullard, J. F., Kale, A. and Baker, N. E. (2009). Clearance of apoptotic corpses. *Apoptosis* 14, 1029-1037.

Gumienny, T. L., Lambie, E., Hartwieg, E., Horvitz, H. R. and Hengartner, M. O. (1999). Genetic control of programmed cell death in the Caenorhabditis elegans hermaphrodite germline. *Development* 126, 1011-1022.

Gumienny, T. L., Brugnera, E., Tosello-Trampont, A. C., Kinchen, J. M., Haney, L. B., Nishiwaki, K., Walk, S. F., Nemergut, M. E., Macara, I. G., Francis, R. et al. (2001). CED-12/ELMO, a novel member of the CrkII/Dock180/Rac pathway, is required for phagocytosis and cell migration. *Cell* 107, 27-41.

Hanahan, D. and Weinberg, R. A. (2000). The hallmarks of cancer. *Cell* 100, 57-70.

Hoeppner, D. J., Hengartner, M. O. and Schnabel, R. (2001). Engulfment genes cooperate with ced-3 to promote cell death in Caenorhabditis elegans. *Nature* 412, 202-206.

Houlden, H., King, R. H., Wood, N. W., Thomas, P. K. and Reilly, M. M. (2001). Mutations in the 5' region of the myotubularin-related protein 2 (MTMR2) gene in autosomal recessive hereditary neuropathy with focally folded myelin. *Brain* 124, 907-915.

Hsu, T. Y. and Wu, Y. C. (2010). Engulfment of apoptotic cells in C. elegans is mediated by integrin alpha/SRC signaling. *Curr. Biol.* 20, 477-486.

Hurwitz, M. E., Vanderzalm, P. J., Bloom, L., Goldman, J., Garriga, G. and Horvitz, H. R. (2009). Abl kinase inhibits the engulfment of apoptotic [corrected] cells in Caenorhabditis elegans. *PLoS Biol.* 7, e99.

Kamath, R. S. and Ahringer, J. (2003). Genome-wide RNAi screening in Caenorhabditis elegans. *Methods* 30, 313-321.

Ketting, R. F., Haverkamp, T. H., van Luenen, H. G. and Plasterk, R. H. (1999). Mut-7 of C. elegans, required for transposon silencing and RNA interference, is a homolog of Werner syndrome helicase and RNaseD. *Cell* 99, 133-141.

Kinchen, J. M. (2010). A model to die for: signaling to apoptotic cell removal in worm, fly and mouse. *Apoptosis* 15, 998-1006.

Kinchen, J. M., Cabello, J., Klingele, D., Wong, K., Feichtinger, R., Schnabel, H., Schnabel, R. and Hengartner, M. O. (2005). Two pathways converge at CED-10 to mediate actin rearrangement and corpse removal in C. elegans. *Nature* 434, 93-99.

Kinchen, J. M., Doukoumetzidis, K., Almendinger, J., Stergiou, L., Tosello-Trampont, A., Sifri, C. D., Hengartner, M. O. and Ravichandran, K. S.

(2008). A pathway for phagosome maturation during engulfment of apoptotic cells. *Nat. Cell Biol.* **10**, 556-566.

Kiyokawa, E., Hashimoto, Y., Kobayashi, S., Sugimura, H., Kurata, T. and Matsuda, M. (1998). Activation of Rac1 by a Crk SH3-binding protein, DOCK180. *Genes Dev.* **12**, 3331-3336.

Kritikou, E. A., Milstein, S., Vidalain, P. O., Lettre, G., Bogan, E., Doukoumetzidis, K., Gray, P., Chappell, T. G., Vidal, M. and Hengartner, M. O. (2006). C. elegans GLA-3 is a novel component of the MAP kinase MPK-1 signaling pathway required for germ cell survival. *Genes Dev.* **20**, 2279-2292.

Laporte, J., Blondeau, F., Buj-Bello, A. and Mandel, J. L. (2001). The myotubularin family: from genetic disease to phosphoinositide metabolism. *Trends Genet.* **17**, 221-228.

Laporte, J., Blondeau, F., Gansmuller, A., Lutz, Y., Vonesch, J. L. and Mandel, J. L. (2002a). The PtdIns3P phosphatase myotubularin is a cytoplasmic protein that also localizes to Rac1-inducible plasma membrane ruffles. *J. Cell Sci.* **115**, 3105-3117.

Laporte, J., Liaubet, L., Blondeau, F., Tronchere, H., Mandel, J. L. and Payrastre, B. (2002b). Functional redundancy in the myotubularin family. *Biochem. Biophys. Res. Commun.* **291**, 305-312.

Laporte, J., Bedez, F., Bolino, A. and Mandel, J. L. (2003). Myotubularins, a large disease-associated family of cooperating catalytically active and inactive phosphoinositides phosphatases. *Hum. Mol. Genet.* **12 Spec No 2**, R285-R292.

Lemmon, M. A. (2008). Membrane recognition by phospholipid-binding domains. *Nat. Rev. Mol. Cell Biol.* **9**, 99-111.

Lettre, G., Kritikou, E. A., Jaeggi, M., Calixto, A., Fraser, A. G., Kamath, R. S., Ahringer, J. and Hengartner, M. O. (2004). Genome-wide RNAi identifies p53-dependent and -independent regulators of germ cell apoptosis in C. elegans. *Cell Death Differ.* **11**, 1198-1203.

Leverrier, Y., Okkenhaug, K., Sawyer, C., Bilancio, A., Vanhaesebroeck, B. and Ridley, A. J. (2003). Class I phosphoinositide 3-kinase p110beta is required for apoptotic cell and Fcgamma receptor-mediated phagocytosis by macrophages. *J. Biol. Chem.* **278**, 38437-38442.

Liu, Q. A. and Hengartner, M. O. (1998). Candidate adaptor protein CED-6 promotes the engulfment of apoptotic cells in C. elegans. *Cell* **93**, 961-972.

Liu, Y. Q., You, S., Tashiro, S., Onodera, S. and Ikejima, T. (2005). Activation of phosphoinositide 3-kinase, protein kinase C, and extracellular signal-regulated kinase is required for oridonin-enhanced phagocytosis of apoptotic bodies in human macrophage-like U937 cells. *J. Pharmacol. Sci.* **98**, 361-371.

Metzstein, M. M., Stanfield, G. M. and Horvitz, H. R. (1998). Genetics of programmed cell death in C. elegans: past, present and future. *Trends Genet.* **14**, 410-416.

Michell, R. H., Heath, V. L., Lemmon, M. A. and Dove, S. K. (2006). Phosphatidylinositol 3,5-bisphosphate: metabolism and cellular functions. *Trends Biochem. Sci.* **31**, 52-63.

Nagata, S., Hanayama, R. and Kawane, K. (2010). Autoimmunity and the clearance of dead cells. *Cell* **140**, 619-630.

Neukomm, L. J., Frei, A. P., Cabello, J., Kinchen, J. M., Zaidel-Bar, R., Ma, Z., Haney, L. B., Hardin, J., Ravichandran, K. S., Moreno, S. et al. (2011). Loss of the RhoGAP SRGP-1 promotes the clearance of dead and injured cells in Caenorhabditis elegans. *Nat. Cell Biol.* **13**, 79-86.

Nicot, A. S. and Laporte, J. (2008). Endosomal phosphoinositides and human diseases. *Traffic* **9**, 1240-1249.

Nieto, C., Almendinger, J., Gysi, S., Gomez-Orte, E., Kaech, A., Hengartner, M. O., Schnabel, R., Moreno, S. and Cabello, J. (2010). ccz-1 mediates the digestion of apoptotic corpses in C. elegans. *J. Cell Sci.* **123**, 2001-2007.

Park, D., Tosello-Trampont, A., Elliott, M. R., Lu, M., Haney, L., Ma, Z., Klibanov, A. L., Mandell, J. W. and Ravichandran, K. (2007). BAI1 is an engulfment receptor for apoptotic cells upstream of the ELMO/Dock180/Rac module. *Nature* **450**, 430-434.

Ravichandran, K. S. and Lorenz, U. (2007). Engulfment of apoptotic cells: signals for a good meal. *Nat. Rev. Immunol.* **7**, 964-974.

Reddien, P. W. and Horvitz, H. R. (2000). CED-2/CrkII and CED-10/Rac control phagocytosis and cell migration in Caenorhabditis elegans. *Nat. Cell Biol.* **2**, 131-136.

Reddien, P. W., Cameron, S. and Horvitz, H. R. (2001). Phagocytosis promotes programmed cell death in C. elegans. *Nature* **412**, 198-202.

Robinson, F. L. and Dixon, J. E. (2006). Myotubularin phosphatases: policing 3-phosphoinositides. *Trends Cell Biol.* **16**, 403-412.

Rohde, H. M., Tronchere, H., Payrastre, B. and Laporte, J. (2009). Detection of myotubularin phosphatases activity on phosphoinositides in vitro and ex vivo. *Methods Mol. Biol.* **462**, 265-278.

Rual, J. F., Klitgord, N. and Achaz, G. (2007). Novel insights into RNAi off-target effects using C. elegans paralogs. *BMC Genomics* **8**, 106.

Saarikangas, J., Zhao, H. and Lappalainen, P. (2010). Regulation of the actin cytoskeleton-plasma membrane interplay by phosphoinositides. *Physiol. Rev.* **90**, 259-289.

Savill, J. and Fadok, V. (2000). Corpse clearance defines the meaning of cell death. *Nature* **407**, 784-788.

Schaletzky, J., Dove, S. K., Short, B., Lorenzo, O., Clague, M. J. and Barr, F. A. (2003). Phosphatidylinositol-5-phosphate activation and conserved substrate specificity of the myotubularin phosphatidylinositol 3-phosphatases. *Curr. Biol.* **13**, 504-509.

Schnabel, R., Hutter, H., Moerman, D. and Schnabel, H. (1997). Assessing normal embryogenesis in Caenorhabditis elegans using a 4D microscope: variability of development and regional specification. *Dev. Biol.* **184**, 234-265.

Senderek, J., Bergmann, C., Weber, S., Ketelsen, U. P., Schorle, H., Rudnik-Schoneborn, S., Buttner, R., Buchheim, E. and Zerres, K. (2003). Mutation of the SBF2 gene, encoding a novel member of the myotubularin family, in Charcot-Marie-Tooth neuropathy type 4B2/11p15. *Hum. Mol. Genet.* **12**, 349-356.

Sijen, T., Fleenor, J., Simmer, F., Thijssen, K. L., Parrish, S., Timmons, L., Plasterk, R. H. and Fire, A. (2001). On the role of RNA amplification in dsRNA-triggered gene silencing. *Cell* **107**, 465-476.

Simonsen, A., Wurmser, A. E., Emr, S. D. and Stenmark, H. (2001). The role of phosphoinositides in membrane transport. *Curr. Opin. Cell Biol.* **13**, 485-492.

Spieth, J., Brooke, G., Kuersten, S., Lea, K. and Blumenthal, T. (1993). Operons in C. elegans: polycistronic mRNA precursors are processed by trans-splicing of SL2 to downstream coding regions. *Cell* **73**, 521-532.

Stanfield, G. M. and Horvitz, H. R. (2000). The ced-8 gene controls the timing of programmed cell deaths in C. elegans. *Mol. Cell* **5**, 423-433.

Sulston, J. E., Schierenberg, E., White, J. G. and Thomson, J. N. (1983). The embryonic cell lineage of the nematode Caenorhabditis elegans. *Dev. Biol.* **100**, 64-119.

Taylor, G. S., Maehama, T. and Dixon, J. E. (2000). Inaugural article: myotubularin, a protein tyrosine phosphatase mutated in myotubular myopathy, dephosphorylates the lipid second messenger, phosphatidylinositol 3-phosphate. *Proc. Natl. Acad. Sci. USA* **97**, 8910-8915.

Tronchere, H., Laporte, J., Pendaries, C., Chaussade, C., Liaubet, L., Pirola, L., Mandel, J. L. and Payrastre, B. (2004). Production of phosphatidylinositol 5-phosphate by the phosphoinositide 3-phosphatase myotubularin in mammalian cells. *J. Biol. Chem.* **279**, 7304-7312.

Walker, D. M., Urbe, S., Dove, S. K., Tenza, D., Raposo, G. and Clague, M. J. (2001). Characterization of MTMR3. an inositol lipid 3-phosphatase with novel substrate specificity. *Curr. Biol.* **11**, 1600-1605.

Wang, X., Li, W., Zhao, D., Liu, B., Shi, Y., Chen, B., Yang, H., Guo, P., Geng, X., Shang, Z. et al. (2010). Caenorhabditis elegans transthyretin-like protein TTR-52 mediates recognition of apoptotic cells by the CED-1 phagocyte receptor. *Nat. Cell Biol.* **12**, 655-664.

Wu, Y. C. and Horvitz, H. R. (1998a). C. elegans phagocytosis and cell-migration protein CED-5 is similar to human DOCK180. *Nature* **392**, 501-504.

Wu, Y. C. and Horvitz, H. R. (1998b). The C. elegans cell corpse engulfment gene ced-7 encodes a protein similar to ABC transporters. *Cell* **93**, 951-960.

Xue, Y., Fares, H., Grant, B., Li, Z., Rose, A. M., Clark, S. G. and Skolnik, E. Y. (2003). Genetic analysis of the myotubularin family of phosphatases in Caenorhabditis elegans. *J. Biol. Chem.* **278**, 34380-34386.

Yeung, T., Ozdamar, B., Paroutis, P. and Grinstein, S. (2006). Lipid metabolism and dynamics during phagocytosis. *Curr. Opin. Cell Biol.* **18**, 429-437.

Yu, X., Lu, N. and Zhou, Z. (2008). Phagocytic receptor CED-1 initiates a signaling pathway for degrading engulfed apoptotic cells. *In PLoS Biol.* **6**, e61.

Yu, X., Odera, S., Chuang, C. H., Lu, N. and Zhou, Z. (2006). C. elegans Dynamin mediates the signaling of phagocytic receptor CED-1 for the engulfment and degradation of apoptotic cells. *Dev. Cell* **10**, 743-757.

Zhou, Z., Caron, E., Hartwieg, E., Hall, A. and Horvitz, H. R. (2001a). The C. elegans PH domain protein CED-12 regulates cytoskeletal reorganization via a Rho/Rac GTPase signaling pathway. *Dev. Cell* **1**, 477-489.

Zhou, Z., Hartwieg, E. and Horvitz, H. R. (2001b). CED-1 is a transmembrane receptor that mediates cell corpse engulfment in C. elegans. *Cell* **104**, 43-56.

Zipkin, I. D., Kindt, R. M. and Kenyon, C. J. (1997). Role of a new Rho family member in cell migration and axon guidance in C. elegans. *Cell* **90**, 883-894.

Zou, W., Lu, Q., Zhao, D., Li, W., Mapes, J., Xie, Y. and Wang, X. (2009). Caenorhabditis elegans myotubularin MTM-1 negatively regulates the engulfment of apoptotic cells. *PLoS Genet.* **5**, e1000679.